Study of the transverse mass spectra of strange particles in Pb-Pb collisions at 158 A GeV/c

The NA57 Collaboration:
F Antinori[l], P Bacon[e], A Badalà[g], R Barbera[g], A Belogianni[a], A Bhasin[e], I J Bloodworth[e], M Bombara[i], G E Bruno[b] †, S A Bull[e], R Caliandro[b], M Campbell[h], W Carena[h], N Carrer[h], R F Clarke[e], A Dainese[l], A P de Haas[s], P C de Rijke[s], D Di Bari[b], S Di Liberto[o], R Divià[h], D Elia[b], D Evans[e], G A Feofilov[q], R A Fini[b], P Ganoti[a], B Ghidini[b], G Grella[p], H Helstrup[d], K F Hetland[d], A K Holme[k], A Jacholkowski[g], G T Jones[e], P Jovanovic[e], A Jusko[e], R Kamermans[s], J B Kinson[e], K Knudson[h], A A Kolozhvari[q], V Kondratiev[q], I Králik[i], A Kravčáková[j], P Kuijer[s], V Lenti[b], R Lietava[e], G Løvhøiden[k], V Manzari[b], G Martinská[j], M A Mazzoni[o], F Meddi[o], A Michalon[r], M Morando[l], E Nappi[b], F Navach[b], P I Norman[e], A Palmeri[g], G S Pappalardo[g], B Pastirčák[i], J Pišút[f], N Pišútová[f], R J Platt[e], F Posa[b], E Quercigh[l], F Riggi[g], D Röhrich[c], G Romano[p], K Šafařík[h], L Šándor[i], E Schillings[s], G Segato[l], M Sené[m], R Sené[m], W Snoeys[h], F Soramel[l] ‡, M Spyropoulou-Stassinaki[a], P Staroba[n], T A Toulina[q], R Turrisi[l], T S Tveter[k], J Urbán[j], F F Valiev[q], A van den Brink[s], P van de Ven[s], P Vande Vyvre[h], N van Eijndhoven[s], J van Hunen[h], A Vascotto[h], T Vik[k], O Villalobos Baillie[e], L Vinogradov[q], T Virgili[p], M F Votruba[e], J Vrláková[j] and P Závada[n]

[a] Physics Department, University of Athens, Athens, Greece
[b] Dipartimento IA di Fisica dell'Università e del Politecnico di Bari and INFN, Bari, Italy
[c] Fysisk Institutt, Universitetet i Bergen, Bergen, Norway
[d] Høgskolen i Bergen, Bergen, Norway
[e] University of Birmingham, Birmingham, UK
[f] Comenius University, Bratislava, Slovakia
[g] University of Catania and INFN, Catania, Italy
[h] CERN, European Laboratory for Particle Physics, Geneva, Switzerland
[i] Institute of Experimental Physics, Slovak Academy of Science, Košice, Slovakia
[j] P.J. Šafárik University, Košice, Slovakia
[k] Fysisk Institutt, Universitetet i Oslo, Oslo, Norway

† To whom correspondence should be addressed (giuseppe.bruno@cern.ch)
‡ Permanent address: University of Udine, Udine, Italy

[l] University of Padua and INFN, Padua, Italy
[m] Collège de France, Paris, France
[n] Institute of Physics, Prague, Czech Republic
[o] University "La Sapienza" and INFN, Rome, Italy
[p] Dipartimento di Scienze Fisiche "E.R. Caianiello" dell'Università and INFN, Salerno, Italy
[q] State University of St. Petersburg, St. Petersburg, Russia
[r] IReS/ULP, Strasbourg, France
[s] Utrecht University and NIKHEF, Utrecht, The Netherlands

Abstract. The NA57 experiment has collected high statistics, high purity samples of K^0_S and Λ, Ξ and Ω hyperons produced in Pb-Pb collisions at 158 A GeV/c. In this paper we present a study of the transverse mass spectra of these particles for a sample of events corresponding to the most central 53% of the inelastic Pb-Pb cross-section. We analyse the transverse mass distributions in the framework of the blast-wave model for the full sample and, for the first time at the SPS, as a function of the event centrality.

PACS numbers: 12.38.Mh, 25.75.Nq, 25.75.Ld, 25.75.Dw

Submitted to: *J. Phys. G: Nucl. Phys.*

1. Introduction

The study of ultrarelativistic heavy-ion collisions is motivated mainly by the quantum chromodynamics (QCD) prediction that at sufficiently high energy density the excited nuclear matter undergoes a phase transition into a system of deconfined quarks and gluons (quark-gluon plasma, QGP) [1].

Strange particles have proved over the past years to be a powerful tool for the study of reaction dynamics in high-energy heavy-ion collisions.
The WA97 experiment has measured [2] an enhanced production of particles carrying one, two or three units of strangeness in central Pb-Pb collisions at 158 A GeV/c with respect to proton induced reactions (strangeness enhancement). The observed pattern of the enhancements as a function of strangeness was predicted more than 20 years ago to be a consequence of a QGP formation [3].

NA57 is a dedicated experiment at the CERN SPS for the study of the production of strange and multi-strange particles in Pb-Pb collisions [4]. It continues and extends the study initiated by its predecessor WA97, by *(i)* enlarging the triggered fraction of the inelastic cross-section thus extending the centrality range towards less central collisions and *(ii)* collecting data also at lower (40 A GeV/c) beam momentum in order to study the energy dependence of the strangeness enhancements.

In this paper we concentrate on the analysis of the transverse mass ($m_{\mathrm{T}} = \sqrt{p_{\mathrm{T}}^2 + m^2}$) spectra for Λ, Ξ^-, Ω^- hyperons, their antiparticles and $\mathrm{K}^0_{\mathrm{S}}$ measured in Pb-Pb collisions at 158 A GeV/c.

The m_{T} spectra are expected to be sensitive to the details of the production dynamics [5, 6]. In particular, for a fireball in local thermal equilibrium, the shapes of the m_{T} spectra depend both on the thermal motion of the particles and on the collective flow driven by the pressure. To disentangle the two contributions, namely thermal motion and transverse flow, one has to rely on models. Several freeze-out scenarios have been proposed (for an overview refer to [7]). They differ in the freeze-out geometry and in the flow velocity profile. In the present analysis we consider the *blast-wave* model [5, 6], which assumes cylindrical symmetry for an expanding fireball in local thermal equilibrium, with different hypotheses on the transverse flow profile.

The paper is organized as follows. The NA57 apparatus is briefly described in section 2. Section 3 deals with the measurements of the transverse mass spectra. Inverse slope parameters are presented and discussed in section 4. The blast-wave model is introduced in section 5 and compared to data under different conditions. Finally, conclusions are drawn in section 6.

2. The NA57 experiment

The NA57 apparatus, schematically shown in figure 1, has been described in detail elsewhere [8]. The Λ, Ξ^-, Ω^- hyperons, their antiparticles and the $\mathrm{K}^0_{\mathrm{S}}$ mesons are identified by reconstructing their weak decays into final states containing only charged

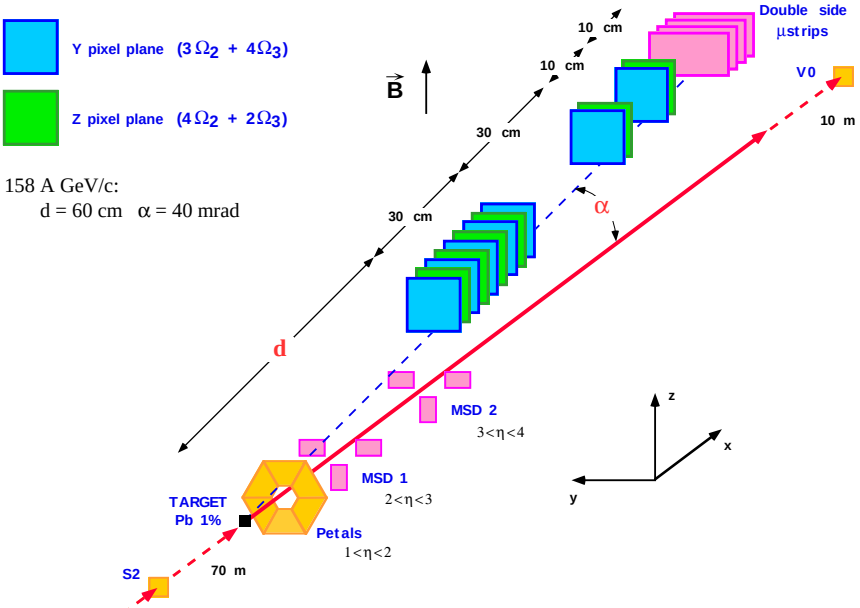

Figure 1. The NA57 apparatus placed inside the 1.4 T field of the GOLIATH magnet.

particles:

$$\begin{aligned} \mathrm{K}^0_{\mathrm{S}} &\rightarrow \pi^+ + \pi^- & \Lambda &\rightarrow p + \pi^- \\ \Xi^- &\rightarrow \Lambda + \pi^- & \Omega^- &\rightarrow \Lambda + K^- \\ &\quad \hookrightarrow p + \pi^- & &\quad \hookrightarrow p + \pi^- \end{aligned} \tag{1}$$

and the corresponding charge conjugates for antihyperons.

Tracks are measured in the silicon tracking telescope, an array of pixel detector planes with 5×5 cm^2 cross-section, with a total length of about 30 cm. To improve the momentum resolution of high momentum tracks a lever arm detector — an array of additional pixel planes and double-sided silicon microstrip detectors — is placed downstream of the tracking telescope. The whole silicon telescope is placed in a 1.4 Tesla magnetic field, above the beam line, inclined and aligned with the lower edge of the detectors laying on a line pointing back to the target. The inclination angle α with respect to the beam line and the distance d of the first pixel plane from the target are set to accept particles produced in about half a unit of rapidity around central rapidity and medium transverse momentum: $\alpha = 40$ mrad and $d = 60$ cm.

An array of scintillation counters (Petals), placed 10 cm downstream of the target, provides a fast signal to trigger on the centrality of the collisions. The triggered fraction of the Pb-Pb inelastic cross-section is about 60%. The centrality of the Pb-Pb collisions is determined (off-line) by analyzing the charged particle multiplicity measured by two stations of silicon strip detectors (MSD) which sample the pseudorapidity intervals $2 < \eta < 3$ and $3 < \eta < 4$.

3. Data analysis

The results presented in this paper are based on the analysis of the full data sample consisting of 460 M events of Pb-Pb collisions.
The strange particle signals are extracted using geometric and kinematic constraints, with a method similar to that used in the WA97 experiment [9]. As an example of the quality of the NA57 data, the invariant mass spectra for $\pi^+\pi^-$, pπ, $\Lambda\pi$ and ΛK after all analysis cuts are shown in figure 2. Hyperon and K^0_S peaks are well centered at the

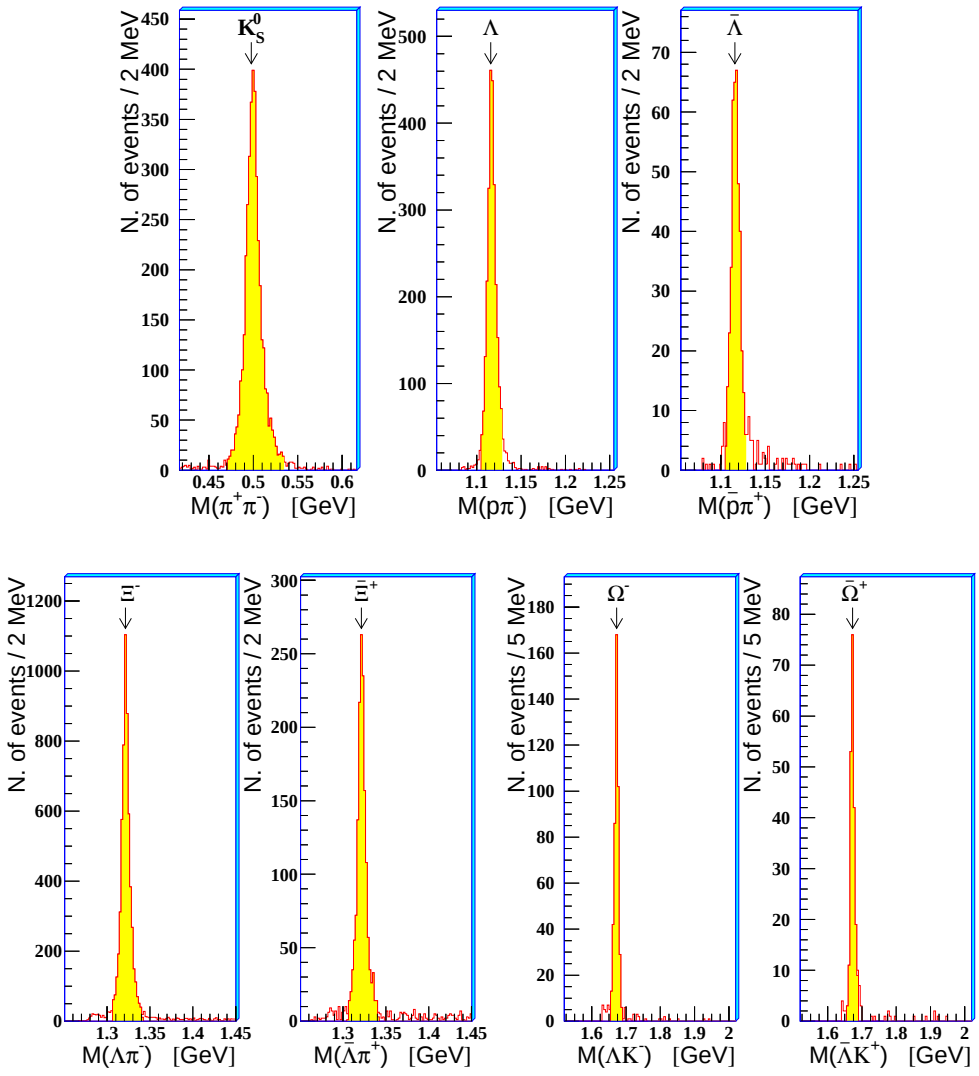

Figure 2. Sample invariant mass spectra for $\pi^+\pi^-$, pπ, $\Lambda\pi$ and ΛK.

PDG values [10] with FWHM of about 10 MeV (15 MeV for the K^0_S).

Although the mass spectra show very low background, a detailed study of the residual combinatorial background has been performed for the high statistics samples (K^0_S, Λ and $\overline{\Lambda}$) using the method of *event mixing*. Fake Λ, $\overline{\Lambda}$ or K^0_S (V^0) candidates are built by pairing all the negative particles from one event with all the positive ones from

a different event, selecting events which are close in multiplicity. Then the fake V^0s from mixed events are processed with reconstruction and analysis programs, like real events. In this way we obtain a good description of the combinatorial background. The absolute normalization is fixed by the number of pairs of oppositely charged particles in real and mixed events. Figure 3 shows the $\pi^+\pi^-$ invariant mass distribution for real and mixed events before (left) and after (right) the application of the analysis cuts. The

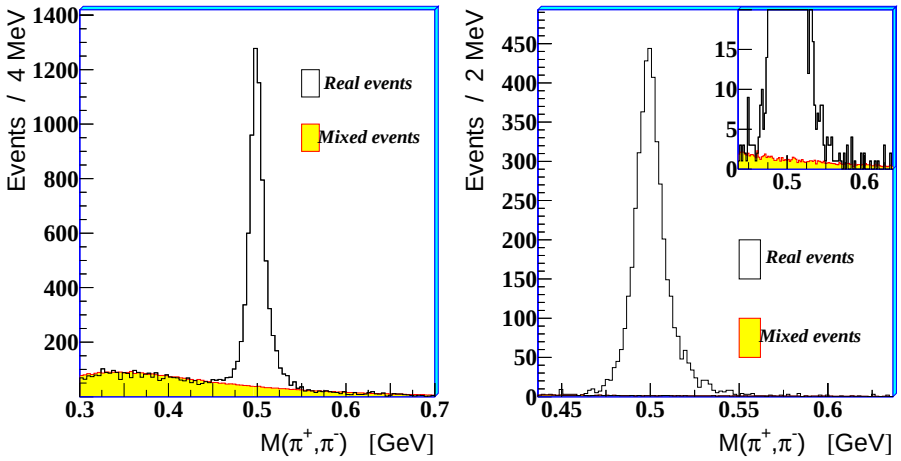

Figure 3. The $\pi^+\pi^-$ invariant mass distribution for real and mixed events before analysis cuts (left) and after analysis cuts (right). The inset in the right plot is a zoom on the vertical axis.

total amount of combinatorial background is estimated to be 0.7%, 0.3% and 1.2% for K^0_S, Λ and $\overline{\Lambda}$, respectively. We therefore neglect it. Additional details of this method can be found in reference [11].
The estimates of the Ξ and Ω background, evaluated with a similar technique, are less than 4% and 6%, respectively. They have also been neglected for this analysis.

For each particle species we define the fiducial acceptance window using a Monte Carlo simulation of the apparatus, in order to exclude the borders where the systematic errors are more difficult to evaluate. The acceptance regions are shown in figure 4. For all hyperons, the acceptance window for particle and antiparticle are the same, due to the reflection symmetry of our apparatus with respect to the magnetic field direction. As a further check, the orientation of the magnetic field was periodically inverted.

All data are corrected for geometrical acceptance and for detector and reconstruction inefficiencies on a event by event basis, with the following procedure:

- for each reconstructed particle a sample of Monte Carlo particles is generated with the same measured rapidity y and transverse momentum p_T, random azimuthal angle and the primary vertex position generated randomly within the target according to the measured beam profile;
- the Monte Carlo particles are traced through a simulation of the apparatus § based

§ Silicon pixel detector efficiencies are accounted for chip-by-chip. Each chip contains 2032 or 1006

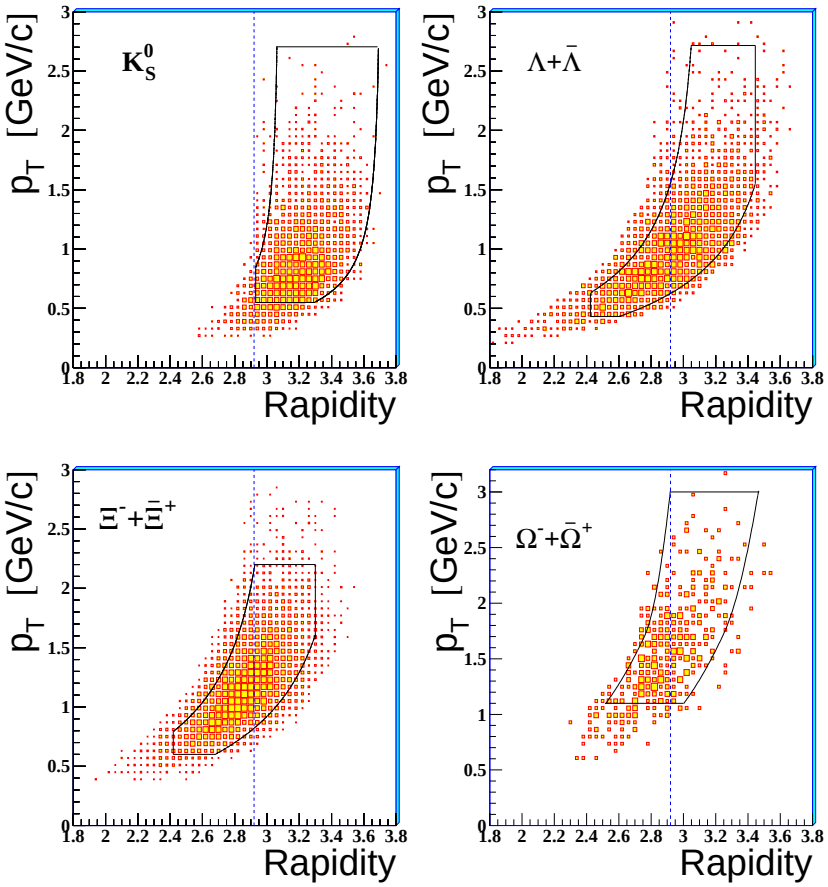

Figure 4. The y–p_T acceptance windows superimposed to the data samples. Dashed lines show the position of mid-rapidity ($y_{cm} = 2.92$).

on GEANT [12] allowing them to decay according to their life times and random internal decay angles.

- the hits of the decay tracks are merged with those of a real event — with a hit multiplicity close to that of the original event — in order to account for background tracks and electronic noise;
- the merged event is processed through the NA57 reconstruction and analysis chain;
- the weight to be associated with the real event is calculated as the ratio of the number of Monte Carlo generated events to the number of Monte Carlo events successfully reconstructed and retained by all analysis selection criteria.

It has been checked that the final weights are not sensitive to the experimental smearing in p_T and y.

The simulation used for calculating the correction factors has been checked in detail [13] by comparing real and Monte Carlo distributions for several parameters, and they show good agreement. As an example, we show in figure 5 three such distributions for each

sensitive cells (pixels) where the pixel size is, respectively, 50×500 μm^2 or 75×500 μm^2 [8].

particle species.

The systematic errors on the inverse slopes have been estimated to be about 10% for all the strange particles.

The weighting method described above is CPU intensive; therefore, while each of the reconstructed Ξs and Ωs have been individually weighted, for the much more abundant K^0_S, Λ and $\overline{\Lambda}$ samples we only weighted a small fraction of the total sample in order to reach a statistical accuracy better than the limits imposed by the systematic error. Table 1 shows the strange particle samples collected by NA57 and those used for the present analysis.

Table 1. Statistics of the strange particle samples used in this analysis (individually *weighted*) and *collected* by NA57 in Pb-Pb collisions at 158 A GeV/c.

Particle	K^0_S	Λ	$\overline{\Lambda}$	Ξ^-	$\overline{\Xi}^+$	Ω^-	$\overline{\Omega}^+$
weighted	3340	2350	2718	5858	1522	432	192
collected	$\times$400	$\times$400	$\times$50	$\times$1	$\times$1	$\times$1	$\times$1

The charged particle multiplicity distribution, which is shown in figure 6, has been divided into five centrality classes (0,1,2,3,4), class 0 being the most peripheral and class 4 the most central. The drop at low multiplicities is due to the centrality selection applied at the trigger level. The fractions of the inelastic cross-section for the five classes, calculated assuming a total cross section of 7.26 barn, are given in table 2.

Table 2. Centrality ranges for the five classes defined in figure 6.

Class	0	1	2	3	4
σ/σ_{inel} (%)	53–40	40–23	23–11	11–4.5	4.5–0

The procedure for the measurement of the multiplicity distribution and the determination of the collision centrality for each class is described in reference [14].

4. Inverse slopes of the transverse mass spectra

The double-differential $(y, m_{\rm T})$ distribution for each particle species has been parametrized using the expression

$$\frac{d^2N}{m_{\rm T}\, dm_{\rm T} dy} = f(y)\ \exp\left(-\frac{m_{\rm T}}{T_{app}}\right) \tag{2}$$

assuming the rapidity distribution to be flat within our acceptance region ($f(y) = \text{const}$). The inverse slope parameter T_{app} ("apparent temperature") has been extracted by means of a maximum likelihood fit of equation 2 to the data. As discussed in the next section, this apparent temperature is interpreted as due to the thermal motion

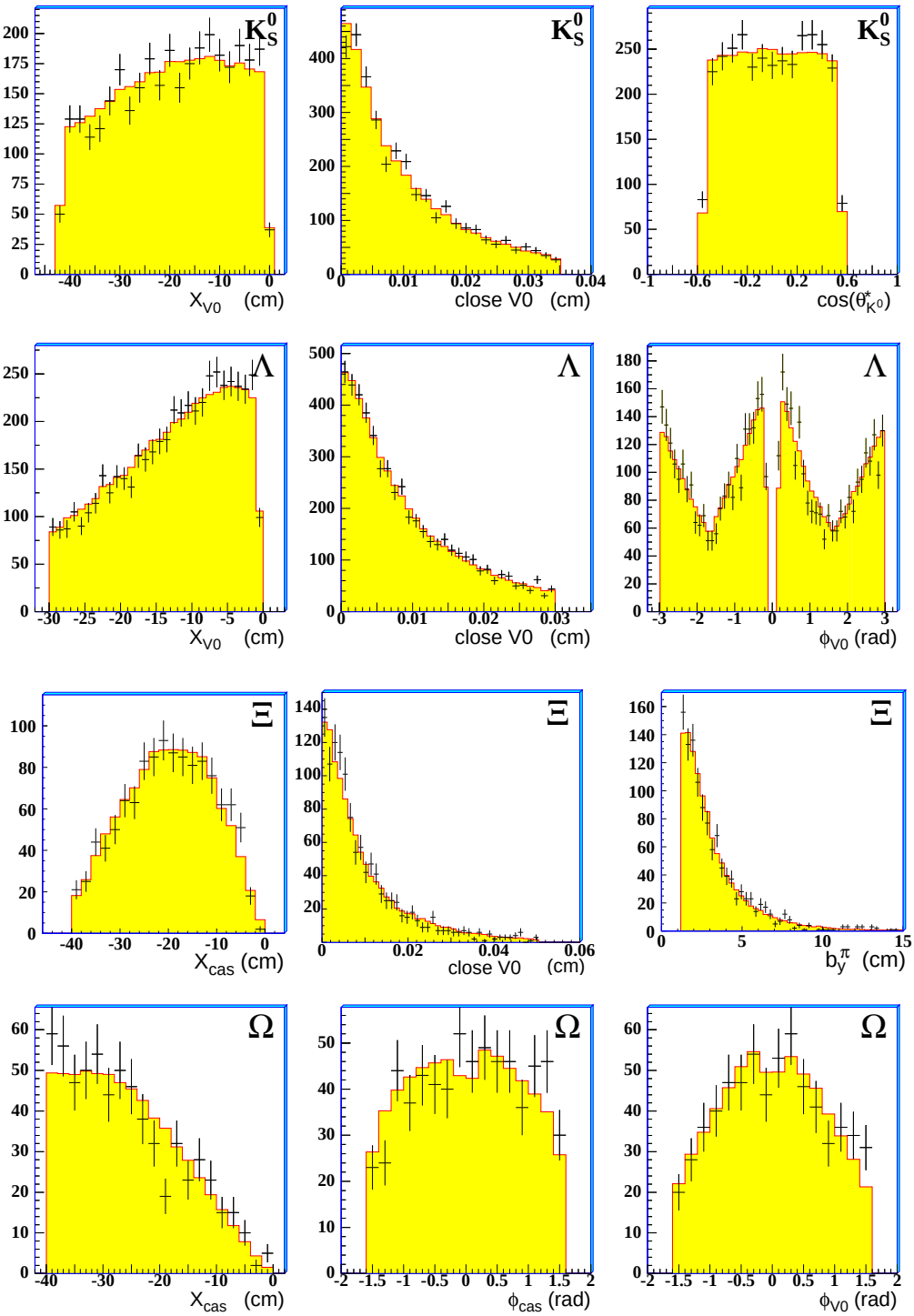

Figure 5. Comparison between real (points with error bars) and Monte Carlo (full lines) distributions. **1st row**, K^0_S: the decay length of the K^0_S; the closest distance in space (*close* parameter) between the extrapolated π^+ and π^- tracks coming from the K^0_S decay; the cosine of θ^*, the angle between the π^- and the K^0_S lines of flight, in the K^0_S reference system. **2nd row**, $\Lambda+\overline{\Lambda}$: the decay length of the Λ; the *close* parameter between the extrapolated p and π; the azimuthal decay angle ϕ. **3rd row**, $\Xi^-+\overline{\Xi}^+$: the decay length of the Ξ; the *close* of the Λ coming from the Ξ; the π impact parameter. **4th row**, $\Omega^-+\overline{\Omega}^+$: the decay length of the Ω; the azimuthal decay angle ϕ in the Ω decay; the azimuthal decay angle ϕ in the subsequent Λ decay.

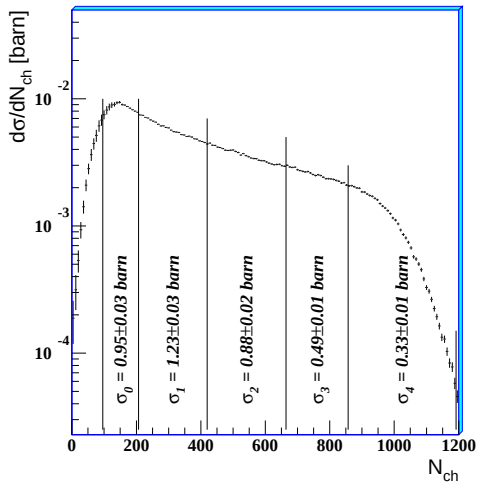

Figure 6. Charged particle multiplicity distribution and limits of the five centrality classes. For each class the corresponding cross-section is indicated.

coupled with a collective transverse flow of the fireball components assumed to be in thermal equilibrium.
In the fits of the Ω^- and $\overline{\Omega}^+$ particle spectra, the lower limit for the accepted transverse momentum was chosen to be 1.4 GeV/c. This choice allows us to exclude a possible instrumental bias at low p_{T} for Ω. The values of the transverse expansion velocity and of the freeze-out temperature obtained within the blast-wave model (see section 5) do not depend significantly on the choice of the lower limit.

The $1/m_{\mathrm{T}}\, dN/dm_{\mathrm{T}}$ distributions for strange particles measured for the full centrality range under consideration are shown in figure 7. The shapes of all spectra are well described by exponential functions. In the next section, we exploit the deviations from the exponential in order to disentangle the transverse flow from the thermal motion. The inverse slope parameters T_{app} of the transverse mass spectra are given in table 3. They are in agreement within the errors with those measured over a smaller centrality range (about the 40% most central inelastic Pb-Pb cross-section) by the WA97 experiment [15].

Table 3. Inverse slope parameter T_{app} (MeV) of the strange particles in the full centrality range (**0-4**). The first error is statistical, the second one systematic.

K^0_S	Λ	$\overline{\Lambda}$
$237 \pm 4 \pm 24$	$289 \pm 7 \pm 29$	$287 \pm 6 \pm 29$

Ξ^-	$\overline{\Xi}^+$	Ω^-	$\overline{\Omega}^+$
$297 \pm 5 \pm 30$	$316 \pm 11 \pm 30$	$264 \pm 19 \pm 27$	$284 \pm 28 \pm 27$

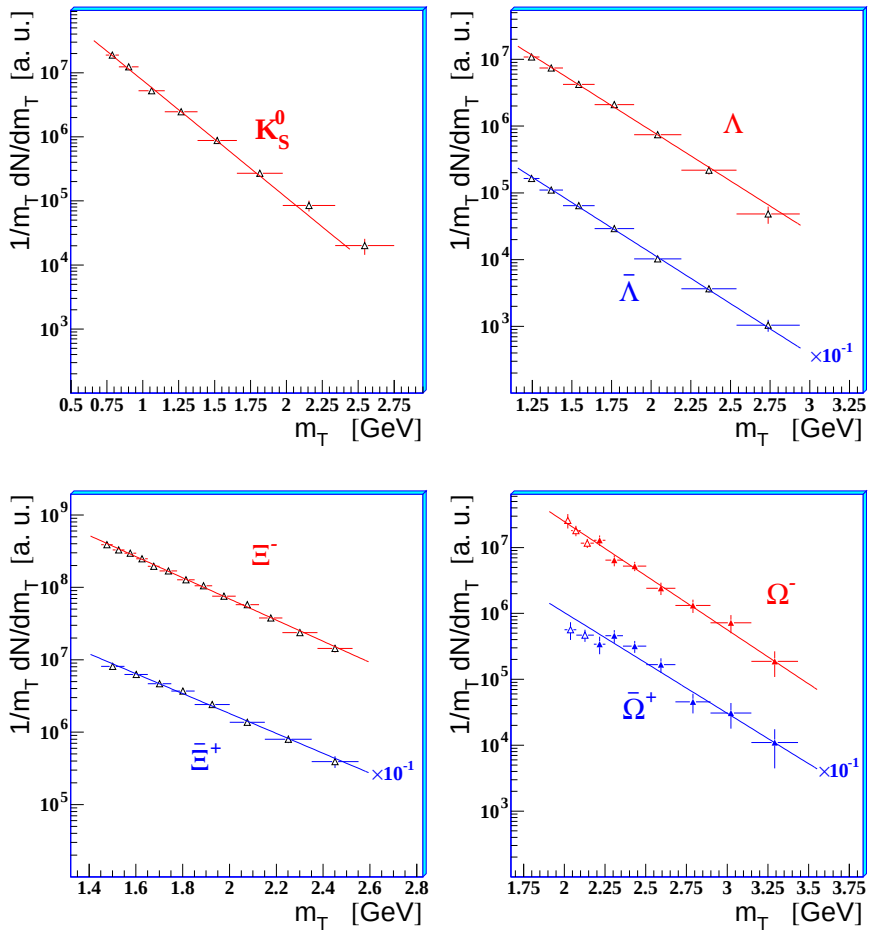

Figure 7. Transverse mass spectra of strange particles for the 53% most central Pb-Pb cross-section. The superimposed exponential functions have inverse slopes equal to the T_{app} values obtained from the maximum likelihood best fits. In the Ω^- and $\overline{\Omega}^+$ spectra, the open points have not been used in the best fit calculation.

A compilation of data‖ on the m_{T} inverse slopes as a function of the particle mass in Pb-Pb interactions at 158 A GeV/c is shown in figure 8.

As already found by the WA97 experiment, the inverse slopes of the Ω hyperon and of the Ξ fall below the line drawn through the π, K and proton points. This observation has been interpreted as due to an early freeze-out of multi-strange hadrons [28].

‖ NA49 results are taken from the following references: π^-, K^- and K^+ from [16]; $\mathrm{K}^0_{\mathrm{S}}$ from [17]; π^+, p and $\overline{\mathrm{p}}$ from [18]; ϕ from [19]; Λ and $\overline{\Lambda}$ from [20]; Ξ^- and $\overline{\Xi}^+$ from [21]; Ω^- and $\overline{\Omega}^+$ from [22]; deuteron from [23]. NA44 results are collected for π^-, π^+, K^-, K^+, p, $\overline{\mathrm{p}}$ from reference [24] and for the deuteron from reference [25]. The point at $m \simeq 3.1$ GeV/c^2 corresponds to the NA50 determination of a thermal spectrum for the J/ψ charmonium state [26]. The J/ψ spectra are fitted using a modified Bessel function, namely $1/T \cdot m_{\mathrm{t}}^2 \cdot K_1(m_{\mathrm{t}}/T)$; this yields an inverse slope $T = 255 \pm 4$ MeV (the value showed in figure 8) for the most central collisions, which is smaller by about 5–10 MeV than the one obtained with the exponential function [26]. Finally the NA50 inverse slopes for the $\rho + \omega$ and ϕ vector-mesons are taken from reference [27].

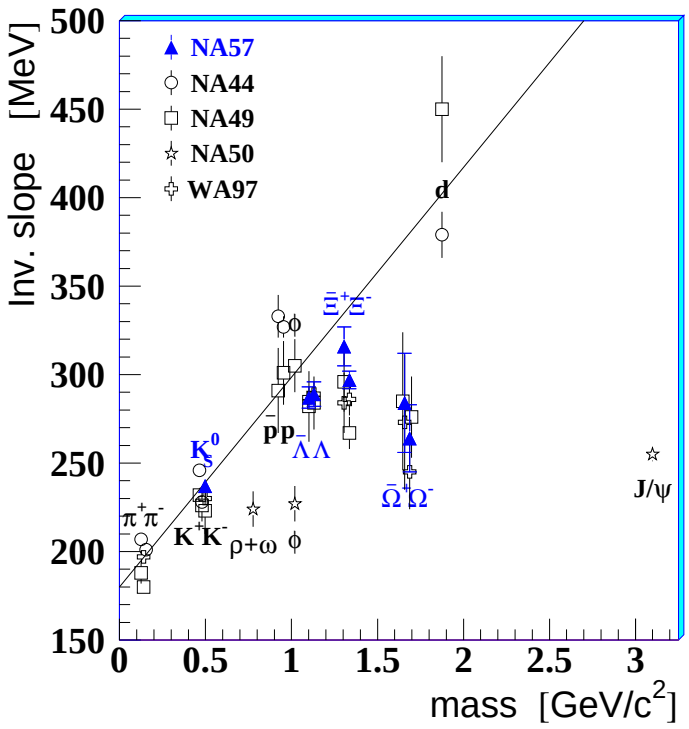

Figure 8. Inverse slopes as a function of the particle rest mass in Pb-Pb interactions at 158 A GeV/c (see text for references). Only statistical errors are shown. The line through π, K and proton is shown to guide the eye.

4.1. Centrality dependence

We have fitted the weighted data by equation 2 separately for each of the five multiplicity classes indicated in figure 6. In order to reduce the statistical errors, the Ω^- and $\overline{\Omega}^+$ samples have been divided into only three centrality classes instead of five: $0+1$, 2 and $3+4$. The $1/m_{\mathrm{T}}\, dN/dm_{\mathrm{T}}$ spectra are shown in figure 9 together with the exponential functions having inverse slopes as obtained from the maximum likelihood fit. The numerical values of the inverse slopes are given in table 4. An increase of the inverse slopes with the centrality is observed in Pb-Pb for Λ, $\overline{\Xi}^+$ and possibly also for $\overline{\Lambda}$.
Inverse slopes for p-Be and p-Pb collisions as measured by WA97 [29] are also given in table 4. In central and semi-central Pb-Pb collisions (i.e. classes 1 to 4) one observes baryon-antibaryon symmetry in the shapes of the spectra: this can be seen in the values of the inverse slopes which are compatible for each hyperon and its antiparticle. This symmetry is not observed in p-Be collisions.
The similarity of baryon and antibaryon m_{T} slopes observed in Pb-Pb suggests that strange baryons and antibaryons are produced by a similar mechanism in nuclear collisions.

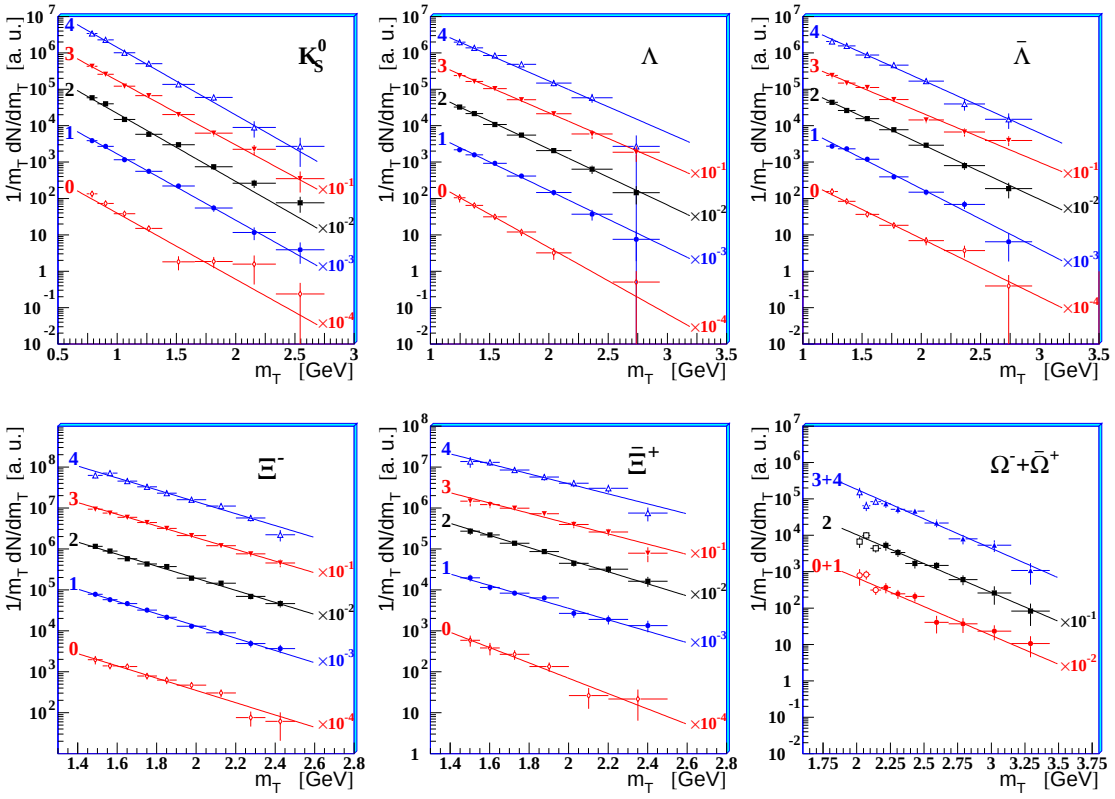

Figure 9. Transverse mass spectra of the strange particles for the five centrality classes of figure 6. For each species, class 4 is displayed uppermost and class 0 lowermost. In the $\Omega^-+\overline{\Omega}^+$ spectra, the open points have not been used in the best fit calculation.

Table 4. Inverse m_T slopes (MeV) of the strange particle distributions for the five Pb-Pb centrality classes, and for p-Be and p-Pb interactions [29]. Only statistical errors are shown. In Pb-Pb, systematic errors are assumed to be independent of centrality.

			Pb-Pb				
	p-Be	p-Pb	0	1	2	3	4
K^0_S	197 ± 4	217 ± 6	239 ± 15	239 ± 8	233 ± 7	244 ± 8	234 ± 9
Λ	180 ± 2	196 ± 6	237 ± 19	274 ± 13	282 ± 12	315 ± 14	305 ± 15
$\overline{\Lambda}$	157 ± 2	183 ± 11	277 ± 19	264 ± 11	283 ± 10	313 ± 14	295 ± 14
Ξ^-	202 ± 13	235 ± 14	290 ± 20	290 ± 11	295 ± 9	304 ± 11	299 ± 12
$\overline{\Xi}^+$	182 ± 17	224 ± 21	232 ± 29	311 ± 23	294 ± 18	346 ± 28	356 ± 31
$\Omega^- + \overline{\Omega}^+$	169 ± 40	334 ± 99	274 ± 34		274 ± 28	268 ± 23	

5. Blast-wave description of the spectra

In this section we use the statistical hadronization model of reference [5] to describe the strange particle spectra discussed above. The model assumes that particles decouple

from a system in local thermal equilibrium with temperature T, which expands both longitudinally and in the transverse direction; the longitudinal expansion is taken to be boost-invariant and the transverse expansion is defined in terms of a transverse velocity field. Finally, the statistical distributions are approximated by the Boltzmann distribution.

The blast-wave model predicts a double differential cross-section for a particle species j of the form:

$$\frac{d^2N_j}{m_{\mathrm{T}}dm_{\mathrm{T}}dy} = \mathcal{A}_j \int_0^{R_G} m_{\mathrm{T}} K_1\left(\frac{m_{\mathrm{T}}\cosh\rho}{T}\right) I_0\left(\frac{p_{\mathrm{T}}\sinh\rho}{T}\right) r\, dr \tag{3}$$

where $\rho(r) = \tanh^{-1}\beta_\perp(r)$, K_1 and I_0 are two modified Bessel functions and $\mathcal{A}_j$ is a normalization constant. With respect to a cylindrical reference system (r,ϕ,z,t), the freeze-out hypersurface is constrained by $0 \leq r \leq R_G$, $0 \leq \phi \leq 2\pi$ and $\partial t_f/\partial r = 0$; the last condition assumes that the particles decouple suddenly from the whole transverse profile of the fireball at time t_f. In these expressions R_G is the transverse geometric radius of the source.

In case of a peripheral collision, the azimuthal symmetry is evidently broken; however it is recovered when considering the m_{T} spectrum of particles accumulated over many events with random impact parameters, which is our approach.

The transverse velocity field $\beta_\perp(r)$ can be parametrized according to a power law:

$$\beta_\perp(r) = \beta_S\left[\frac{r}{R_G}\right]^n \qquad r \leq R_G \tag{4}$$

With this type of profile the numerical value of R_G does not influence the shape of the spectra but just the absolute normalization (i.e. the $\mathcal{A}_j$ constant). Once the transverse flow profile (i.e. equation 4) has been fixed, the shape of each spectrum is determined by the temperature, the velocity of the transverse expansion and the mass of the particle. The parameters which can be extracted from a fit of equation 3 to the experimental spectra are thus the thermal freeze-out temperature T and the surface transverse flow velocity β_S. In order to compare results from different profile hypotheses, corresponding to different values of the exponent n in equation 4, the average transverse flow velocity can be used instead. Assuming a uniform particle density, the average‡ is [30]:

$$< \beta_\perp >= \frac{2}{2+n}\beta_S \tag{5}$$

5.1. Global fits to the spectra using different flow velocity profiles

Preliminary NA57 results of the blast-wave model were presented [31] using a constant ($n = 0$) velocity profile, for the purpose of comparison with the NA49 analysis [32]. In

‡ A more sophisticated averaging can be achieved by incorporating not only the transverse geometry of the model but also the phase space density of particles [30]. According to this definition, $< \beta_\perp >$ is also a function of T and it differs from the values calculated according to equation 5 by 2% if $n = 1/2$, by 5% if $n = 1$ and by 10% if $n = 2$; obviously for $n = 0$, $< \beta_\perp >= \beta_S$ independently of the average definition.

the following, we will adopt primarily the linear ($n = 1$) r-dependence of the transverse flow velocity. In fact, a constant flow profile description of the transverse expansion is internally inconsistent, because the outermost fluid elements of the expanding fireball should have travelled faster than the innermost ones: $\beta(r_1) > \beta(r_2)$ if $r_1 > r_2$. On the other hand, the quadratic profile ($n = 2$) is disfavoured by data, as will be shown below. We also consider the $n = 1/2$ profile which has been suggested to resemble closely the solution of the full hydro-dynamical calculation [33].

The global fit of equation 3 with $n = 1$ to the data points of all the measured strange particle spectra is shown in figure 10; it successfully describes all the distributions with $\chi^2/ndf = 37.2/48$, yielding the following values for the two parameters T and $< \beta_\perp >$:

$$T = 144 \pm 7(\texttt{stat}) \pm 14(\texttt{syst})\text{MeV}\,, \quad < \beta_\perp >= 0.381 \pm 0.013(\texttt{stat}) \pm 0.012(\texttt{syst})\,.$$

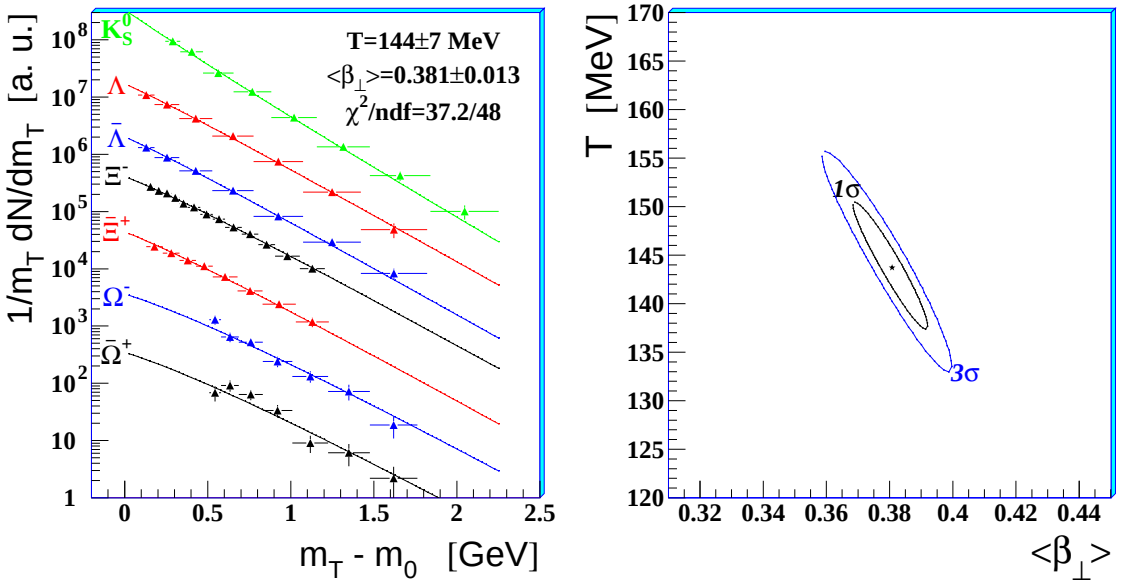

Figure 10. Blast-wave fit to the spectra with a linear profile (left); corresponding 1σ and 3σ confidence level contours in the $< \beta_\perp >$–T plane (right).

The T and $< \beta_\perp >$ parameters are found to be statistically anti-correlated, as can be seen from the confidence level contours shown in figure 10. Conversely, the systematic errors on T and $< \beta_\perp >$ are found to be correlated and they are estimated to be 10% and 3%, respectively.

The results of the fits with all the four profile hypotheses are given in table 5. The three profiles $n = 0$, $n = 1/2$ and $n = 1$ yield similar values of the freeze-out temperatures and of the average transverse flow velocities, with good values of χ^2/ndf. The quadratic profile is disfavoured by our data.

For m_T sufficiently larger than the particle mass m_0, the inverse slope T_{app} is expected to be independent of m_0 [6]. In the non-relativistic regime ($p_\text{T} < m_0$) T_{app} is expected to increase with the rest mass of the particle; e.g. in reference [34] it has

Table 5. Results of the blast-wave model fit using different transverse flow profiles. The quoted errors are statistical. The systematic errors on the temperature and on the velocities are estimated to be about 10% and 3%, respectively, for all the four profiles.

	$n = 0$	$n = 1/2$	$n = 1$	$n = 2$
T (MeV)	158 ± 6	152 ± 6	144 ± 7	151 ± 11
β_S	0.396 ± 0.015	0.493 ± 0.016	0.571 ± 0.019	0.633 ± 0.028
$< \beta_\perp >$	0.396 ± 0.015	0.394 ± 0.013	0.381 ± 0.013	0.316 ± 0.014
χ^2/ndf	39.6/48	36.9/48	37.2/48	68.0/48

been derived that $T_{app} \approx T + \frac{1}{2} m_0 < \beta_\perp >^2$: the larger the mass of the particle the more pronounced the flattening of the spectra at low m_{T}. The deviations from exponential behaviour are larger for large flows and at low m_{T}. Due to its light mass, the $\mathrm{K}^0_{\mathrm{S}}$ spectrum is predicted by the model, and indeed observed, to be steeper at low m_{T}. Such behaviour is illustrated in figure 11 where we compute the "local" inverse slope, i.e. the inverse slope T_{app} of the exponential function $\exp(-m_{\mathrm{T}}/T_{app})$ which is tangent to the blast-wave curve, as a function of $m_{\mathrm{T}} - m_0$. Pions, which in principle would be an even better probe for this behaviour, are unfortunately affected by resonance decays (at low p_{T}) which cannot be neglected [35, 36].

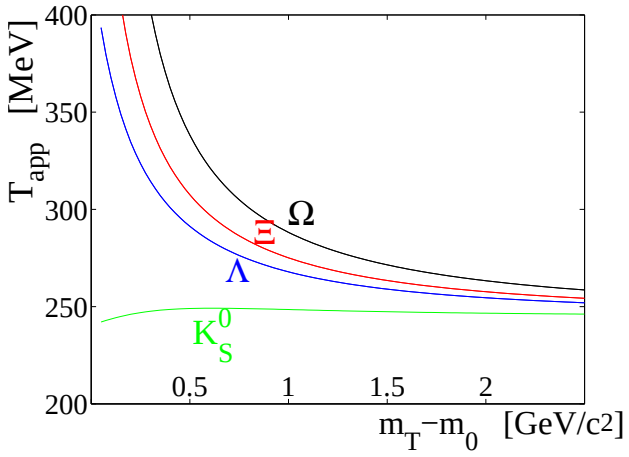

Figure 11. Local inverse slopes according to the blast-wave model using the $n = 1$ transverse profile.

The particles have been divided into two groups — those which share valence quarks with the nucleons and those which do not — since it is known that the particles of the two groups may exhibit different production features. The fit procedure has been repeated separately for the two groups ($n = 1$ case) and the results are given in table 6. They suggest common freeze-out conditions for the two groups. Since the interaction cross-sections for the particles of the two groups are quite different, this finding would

Table 6. Thermal freeze-out temperature (T), surface (β_S) and average ($< \beta_\perp >$) transverse flow velocity in the full centrality range, assuming a linear transverse profile ($n = 1$). The first error is statistical, the second one systematic.

particles	**T** (MeV)	β_S	$< \beta_\perp >$	χ^2/ndf
K^0_S, Λ, Ξ^-	$146 \pm 8 \pm 14$	$0.564 \pm 0.023 \pm 0.018$	$0.376 \pm 0.015 \pm 0.012$	18.1/23
$\overline{\Lambda}$, $\overline{\Xi}^+$, Ω^-, $\overline{\Omega}^+$	$130 \pm 28 \pm 14$	$0.604 \pm 0.048 \pm 0.018$	$0.403 \pm 0.032 \pm 0.012$	18.5/23

suggest limited importance of final state interactions (i.e. a rapid thermal freeze-out) and a similar production mechanism. A similar conclusion concerning the evolution of the system was reached from the study of the HBT correlation functions of negative pions [37, 38, 39].

It has been suggested [28], based on WA97 results on the hyperon $m_{\rm T}$ slopes compatible with those discussed in section 4, that the thermal freeze-out occurs earlier for Ω and possibly for Ξ than for particles of strangeness 0, due to the low scattering cross-sections for Ω and Ξ. The 1σ contours of the separate blast wave fits for singly and multiply strange particles are shown in figure 12. Both groups of particles are compatible with the global-fit determination. However, the fit for the multiply strange particles is statistically dominated by the Ξ; in fact the Ξ+Ω contour remains essentially unchanged when fitting the Ξ alone. Therefore we can only conclude that the Ξ undergoes a thermal freeze-out which is compatible with that of Λ and $\rm K^0_S$.
Due to the lower statistics of the Ω, from its spectrum alone it was not possible to extract significant values for the two freeze-out parameters, as can be done for the Ξ. Any possible deviation of the Ω from the observed common freeze-out undergone by $\rm K^0_S$, Λ and Ξ can only be inferred from the integrated information of the Ω spectrum, i.e. from its inverse slope.

In figure 13 we plot the inverse slopes of figure 8 superimposing the blast-wave model results. The full lines represent the blast-wave calculations when fitting the $m_{\rm T}$ spectrum of a particle, as a function of mass, in the common range $0.05 < m_{\rm T} - m_0 < 1.50$ GeV/c^2, for two different freeze-out conditions: absence of transverse flow ($< \beta_\perp >= 0$) and our best fit determination. The inverse slope is also a function of the $m_{\rm T} - m_0$ range where the fit is performed. This dependence is stronger for heavier particles (see figure 11). Therefore we have also computed the blast-wave inverse slopes of $\rm K^0_S$, Λ, Ξ and Ω spectra in the $m_{\rm T} - m_0$ ranges of NA57 (closed circles in figure 13). The measured inverse slopes of Ω show a deviation from the global trend of the other strange particles.

5.2. Centrality dependence

We have performed the global fit to the spectra for each of the five centrality classes defined in section 3. In figure 14 we show the 1σ confidence level contours in the $< \beta_\perp >$–T plane as obtained for the $n = 1$ profile. The numerical values of the fit

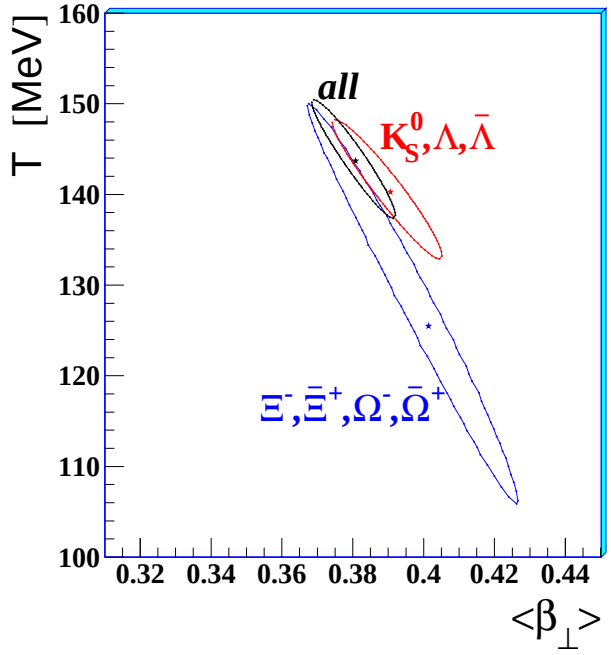

Figure 12. The thermal freeze-out temperature vs average transverse flow for the blast-wave fits ($n = 1$ profile) to multiply and singly strange particle spectra. The 1σ contours are shown, with the marker indicating the optimal fit location. The global fit contour (*all*) is also shown.

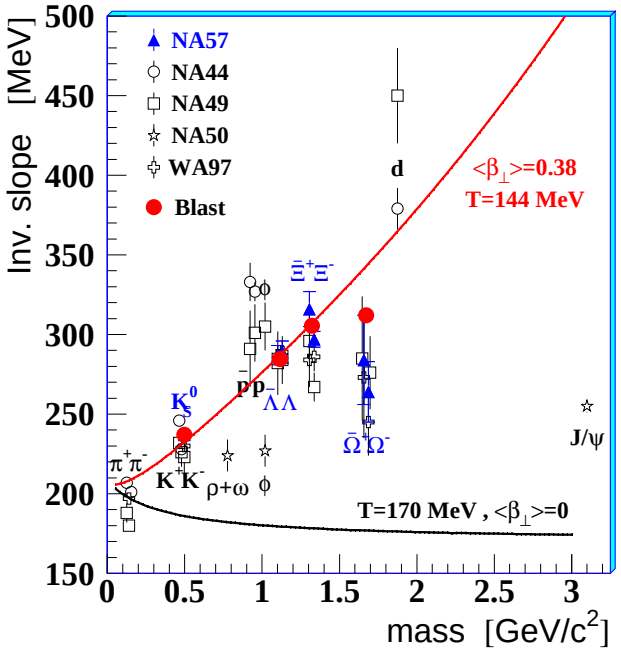

Figure 13. Prediction of the blast-wave model for inverse slopes (see text for details).

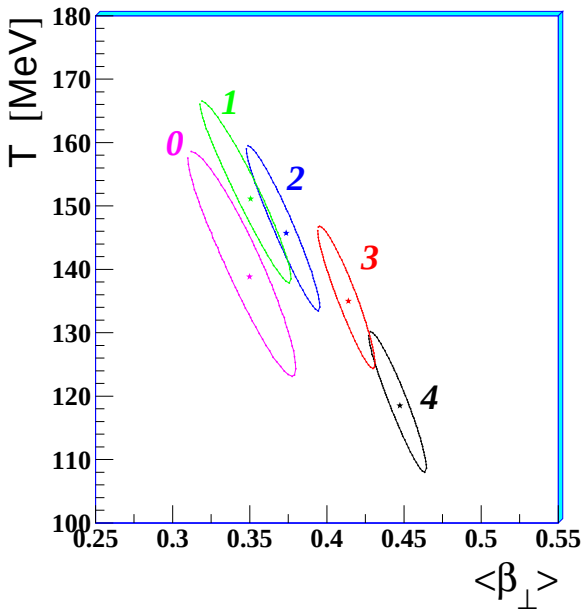

Figure 14. The 1σ confidence level contours from fits in each centrality class.

parameters are given in table 7. The observed trend is as follows: the more central the collisions the larger the transverse collective flow and the lower the final thermal freeze-out temperature. The higher freeze-out temperature for peripheral collisions may be interpreted as the result of an earlier decoupling of the expanding system.

A similar centrality dependence of the freeze-out parameters has been observed by the PHENIX experiment in Au-Au collisions at $\sqrt{s_{NN}} = 130$ GeV from the blast-wave analysis of $\pi^{\pm}$, $K^{\pm}$, p and $\overline{p}$ spectra [40]. In particular, PHENIX has measured‡ $T = 121 \pm 4$ MeV, $< \beta_{\perp} >= 0.47 \pm 0.01$ with $\chi^2/ndf = 34.0/40$ for the most central 5% of the Au-Au cross-section and $T = 140 \pm 4$ MeV, $< \beta_{\perp} >= 0.39 \pm 0.01$ with $\chi^2/ndf = 68.9/40$ for peripheral collisions (30–60% centrality, which corresponds roughly to the NA57 class 0). For the same colliding system, the STAR experiment has also determined [41] the thermal freeze-out for central collisions (see table 7): STAR results would suggest a rather earlier decoupling of the multi-strange Ξ with respect to non strange and singly strange particles at RHIC energy.

We also quote the result of our fit for the most central class, when the $n = 0$ profile is assumed: $T = 134 \pm 10 \pm 13$ MeV, $< \beta_{\perp} >= 0.457 \pm 0.025 \pm 0.014$ and $\chi^2/\mathrm{ndf} = 47.2/43$. This result is found to be consistent within two standard deviations with that from a similar analysis performed by NA49§ assuming the constant profile hypothesis [32].

In table 7 we also make a comparison with results from different measurements which exploit the p_{T} dependence of the HBT correlation functions of negative pions [37, 38, 39]. The thermal freeze-out temperatures and transverse flow velocities are found to be in

‡ In the PHENIX analysis, statistical and systematic errors are added in quadrature before the fit.

§ The NA49 centrality ranges are 0-5% for $K^{\pm}$ and ϕ, 0-10% for π, Λ and Ξ, 0-20% for Ω.

Table 7. Thermal freeze-out temperature and transverse flow velocity in the five centrality classes, assuming a linear transverse profile ($n = 1$). Only statistical errors are quoted; the systematic errors on T and $< \beta_\perp >$ are estimated to be 10% and 3%, respectively. We also give the blast-wave determinations of T and $< \beta_\perp >$ by the NA49 experiment in Pb-Pb collisions at 158 A GeV/c [32], and by the PHENIX and STAR experiments in Au-Au collisions at $\sqrt{s_{NN}} = 130$ GeV [40, 41]. Finally, we quote the measurements by the NA49 [37], WA97 [38] and CERES [39] experiments which use HBT correlation combined with information from h^- and/or deuterium single particle spectra.

Exp.	σ/σ_{inel} %	$\sqrt{s_{NN}}$	technique	**T** (MeV)	$< \beta_\perp >$	χ^2/ndf
NA57	40-53	17.3	this analysis, $n = 1$	139 ± 25	0.35 ± 0.04	33.2/35
NA57	23-40	17.3	this analysis, $n = 1$	151 ± 15	0.35 ± 0.03	42.3/42
NA57	11-23	17.3	this analysis, $n = 1$	146 ± 17	0.37 ± 0.03	41.3/43
NA57	4.5-11	17.3	this analysis, $n = 1$	135 ± 14	0.41 ± 0.02	31.8/41
NA57	0-4.5	17.3	this analysis, $n = 1$	118 ± 13	0.45 ± 0.02	52.7/43
NA49	0-5,10,20	17.3	K^+,p,Λ,Ξ^-,Ω^-, $n = 0$	127 ± 4	0.48 ± 0.01	118/43
NA49	0-5,10,20	17.3	K^-,$\overline{p}$,ϕ,$\overline{\Lambda}$,$\overline{\Xi}^+$,$\overline{\Omega}^+$, $n = 0$	122 ± 2	0.48 ± 0.01	46/41
PHENIX	60-92	130	$\pi^\pm$,$K^\pm$,p,$\overline{p}$, $n = 1$	161^{+19}_{-12}	$0.16^{+0.16}_{-0.2}$	36.3/40
PHENIX	30-60	130	$\pi^\pm$,$K^\pm$,p,$\overline{p}$, $n = 1$	140 ± 4	0.39 ± 0.01	68.9/40
PHENIX	15-30	130	$\pi^\pm$,$K^\pm$,p,$\overline{p}$, $n = 1$	134 ± 2	0.43 ± 0.01	36.2/40
PHENIX	5-15	130	$\pi^\pm$,$K^\pm$,p,$\overline{p}$, $n = 1$	125 ± 2	0.46 ± 0.01	34.7/40
PHENIX	0-5	130	$\pi^\pm$,$K^\pm$,p,$\overline{p}$, $n = 1$	121 ± 4	0.47 ± 0.01	34.0/40
STAR	0-10	130	Ξ^-, $\overline{\Xi}^+$, $n = 1/2$	182 ± 29	0.42 ± 0.06	13/15
STAR	0-10	130	π,K,p,Λ, $n = 1/2$	103 ± 7	0.57 ± 0.01	
NA49	0-3	17.3	HBT + h^- + d	120 ± 12	0.55 ± 0.12	
WA97	25-40	17.3	HBT + h^-	140^{+26}_{-13}	$0.30^{+0.09}_{-0.16}$	
WA97	12-25	17.3	HBT + h^-	121^{+15}_{-11}	$0.47^{+0.07}_{-0.10}$	
WA97	5-12	17.3	HBT + h^-	117^{+16}_{-11}	$0.48^{+0.08}_{-0.11}$	
WA97	0-5	17.3	HBT + h^-	120^{+15}_{-11}	$0.46^{+0.07}_{-0.10}$	
CERES	15-30	17.3	HBT	fixed at 120	$0.49^{+0.06}_{-0.06}$	
CERES	10-15	17.3	HBT	fixed at 120	$0.53^{+0.06}_{-0.05}$	
CERES	5-10	17.3	HBT	fixed at 120	$0.46^{+0.04}_{-0.04}$	
CERES	0-5	17.3	HBT	fixed at 120	$0.55^{+0.03}_{-0.03}$	

good overall agreement with those extracted from the blast-wave fits.

6. Conclusions

We have analysed the transverse mass spectra of high statistics, high purity samples of K^0_S, Λ, Ξ and Ω particles produced in Pb-Pb collisions at 158 A GeV/c over a wide range of collision centrality (the most central 53% of the Pb-Pb inelastic cross-section).

The inverse slopes agree with those measured by WA97. For each hyperon species, the m_T slope is found to be in good agreement with that of the antiparticle. An increase of the inverse slopes with the collision centrality is observed for Λ and $\overline{\Xi}^+$.

The analysis of the transverse mass spectra at 158 A GeV/c in the framework of the blast-wave model suggests that after a central collision the system expands explosively;

the system then freezes-out when the temperature is of the order of 120 MeV with an average transverse flow velocity of about one half of the speed of light. Particles with and without valence quarks in common with the nucleon appear to have a similar behaviour. The inverse slope of the Ω particle deviates from the prediction of the blast-wave model tuned on the other strange particles (K^0_S, Λ and Ξ). Thermal freeze-out conditions (i.e. temperature and transverse flow velocity) are found to be similar to those measured at RHIC energy for singly strange and non strange particles, in both central and peripheral collisions; conversely the temperature measured for the multiply strange Ξ is significantly larger at RHIC. Finally, the results on the centrality dependence of the expansion dynamics indicate that with increasing centrality the transverse flow velocity increases and the final temperature decreases.

Acknowledgments

We are grateful to U Heinz, J Rafelski, B Tomášik and U A Wiedemann for useful comments and fruitful discussions.

References

[1] Cabibbo N and Parisi G 1975 *Phys. Lett.* B **59** 67
[2] Andersen E *et al.* 1999 *Phys. Lett.* B **449** 401
Antinori F *et al.* 1999 *Nucl. Phys.* A **661** 130c
[3] Rafelski J and Müller B 1982 *Phys. Rev. Lett.* **48** 1066
Rafelski J and Müller B 1986 *Phys. Rev. Lett.* **56** 2334
[4] Caliandro R *et al.*, NA57 proposal, 1996 *CERN/SPSLC 96-40, SPSLC/P300*
[5] Schnedermann E, Sollfrank J and Heinz U 1993 *Phys. Rev.* C **48** 2462
[6] Schnedermann E, Sollfrank J and Heinz U 1994 *Phys. Rev.* C **50** 1675
[7] Torrieri G and Rafelski J 2004 *J. Phys. G: Nucl. Phys.* **30** s557
Torrieri G and Rafelski J 2002 *Preprint* nucl-th/0212091
[8] Manzari V *et al.* 1999 *J. Phys. G: Nucl. Phys.* **25** 473
Manzari V *et al.* 1999 *Nucl. Phys.* A **661** 761c
[9] Andersen E *et al.* 1998 *Phys. Lett.* B **433** 209
Lietava R *et al.* 1999 *J. Phys. G: Nucl. Phys.* **25** 181
Fini R A *et al.* 2001 *J. Phys. G: Nucl. Phys.* **27** 375
[10] Hagiwara K *et al.* 2002 *Phys. Rev.* D **66** 010001
[11] Bruno G E *et al.* 2002 *Proceeding of the* 37^{th} *Rencontres de Moriond*, *Preprint* hep-ex/0207047
Bruno G E 2002 *Ph.D. Thesis*, University of Bari (*Preprint* nucl-ex/0402014)
[12] GEANT, CERN Program Library Long Writeup W5013
[13] Fanebust K *et al.* 2002 *J. Phys. G: Nucl. Phys.* **28** 160
[14] Carrer N *et al.* 2001 *J. Phys. G: Nucl. Phys.* **27** 391
[15] Antinori F *et al.* 2000 *Eur. Phys. J.* C **14** 633
[16] Afanasiev S V *et al.* 2002 *Phys. Rev.* C **66** 054902
[17] Margetis S *et al.* 1999 *J. Phys. G: Nucl. Phys.* **25** 189
[18] Afanasiev S V *et al.* 1996 *Nucl. Phys.* A **610** 188
[19] Afanasiev S V *et al.* 2000 *Phys. Lett.* B **491** 59
[20] Alber T *et al.* 1997 *J. Phys. G: Nucl. Phys.* **23** 1817
[21] Afanasiev S V *et al.* 2002 *Phys. Lett.* B **538** 275
[22] Mitrovski M *et al.* 2004 *J. Phys. G: Nucl. Phys.* **30** s357

[23] Afanasiev S V *et al.* 2000 *Phys. Lett.* B **486** 22
[24] Bearden I G *et al.* 2002 *Phys. Rev.* C **66** 044907
[25] Bearden I G *et al.* 2002 *Eur. Phys. J.* C **23** 237
[26] Abreu M C *et al.* 2001 *Phys. Lett.* B **499** 85
[27] Quintans C *et al.* 2001 *J. Phys. G: Nucl. Phys.* **27** 405
[28] van Hecke H, Sorge H and Xu N 1998 *Phys. Rev. Lett.* **81** 5764
[29] Fini R A *et al.* 2001 *Nucl. Phys.* A **681** 141c
[30] Esumi S, Chapman S, van Hecke H and Xu N 1997 *Phys. Rev.* C **55** 2163
[31] Bruno G E 2002 *Ph.D. Thesis*, University of Bari (*Preprint* nucl-ex/0402014)
Bruno G E *et al.* 2003 *Proceeding of the* 38^{th} *Rencontres de Moriond*, *Preprint* nucl-ex/0305033
Šándor L *et al.* 2004 *J. Phys. G: Nucl. Phys.* **30** s129
[32] Van Leeuwen M *et al.* 2003 *Nucl. Phys.* A **715** 165
Friese V *et al.* 2004 *J. Phys. G: Nucl. Phys.* **30** s119
[33] Wiedemann U A, 2003 *private communication*
[34] Lee K S, Heinz U and Schnedermann E 1990 *Z. Phys.* C **48** 525
Csörgő T and Lorstad B 1996 *Phys. Rev.* C **54** 1390
[35] Sollfrank J, Koch P and Heinz U 1990 *Phys. Lett.* **252** 256
[36] Tomášik B, Wiedemann U A and Heinz U 2003 *Heavy Ion Physics* 105
[37] Appelshäuser H et al. 1998 *Eur. Phys. J.* C **2** 661
[38] Antinori F *et al.* 2001 *J. Phys. G: Nucl. Phys.* **27** 2325
[39] Adamová *et al.* 2003 *Nucl. Phys.* A **714** 124
[40] Adcox K *et al.* 2003, *Preprint* nucl-ex/0307010, submitted to *Phys. Rev.* C
[41] Adams J *et al.* 2003, *Preprint* nucl-ex/0307024, *submitted* to *Phys. Rev. Lett.*
Castillo J *et al.* 2004, *J. Phys. G: Nucl. Phys.* **30** s181